Multibody Syst Dyn (2012) 28:21–36
DOI 10.1007/s11044-011-9273-8

The influence of modeling hypothesis and experimental methodologies in the accuracy of muscle force estimation using EMG-driven models

Luciano L. Menegaldo · Liliam F. Oliveira

Received: 29 March 2011 / Accepted: 8 September 2011 / Published online: 10 November 2011

Abstract This paper discusses some methodological questions regarding the application of EMG-driven models to estimate muscle forces, for the *triceps surae* performing isometric contractions. Ankle torque is estimated from a Hill-type muscle model driven by EMG data, collected from the three components of *triceps surae* and *tibialis anterior*. Ankle joint torque is synchronously collected from a dynamometer, which is compared to the sum of each muscle force multiplied by the respective ankle moment arm. A protocol consisting of two steps of low and medium/high loads is used. Raw EMG signal is processed and used as the input signal for the muscle model. The difference between simulated and dynamometer measured torque is calculated as the RMS error between the two curves. A set of *nominal* muscle model parameters is initially chosen from literature (e.g., OpenSim), which allows observing the characteristics of the error distribution. One possibility to improve model accuracy is using individual muscle parameters. We investigated the effect of applying simple scale factors to the nominal muscle model parameters and using ultrasound for estimating muscle maximum force. Other questions regarding muscle model improvements are also addressed, such as using a nonlinear formulation of activation dynamics and variable pennation angle. Surface EMG signals acquisition and processing can also affect force estimation accuracy. Electrodes positioning can influence signal amplitude, and the one-channel EMG may not represent actual excitation for the whole muscle. We have shown that high density EMG reduces, in some cases, the torque estimation error.

Keywords Muscle biomechanics · EMG-driven models · Triceps surae · Plantar flexion

L.L. Menegaldo (✉)
Biomedical Engineering Program, Institute for Graduate Studies and Research in Engineering (COPPE), Federal University of Rio de Janeiro, Av. Horácio Macedo 2030, Bloco H-338, Ilha do Fundão, 21941-914 Rio de Janeiro, Brazil
e-mail: lmeneg@peb.ufrj.br

L.F. Oliveira
School of Physical Education and Sports, Federal University of Rio de Janeiro, Av. Carlos Chagas Filho 540, Ilha do Fundão, 21949-900 Rio de Janeiro, Brazil
e-mail: liliam@eefd.ufrj.br

1 Introduction

Predicting muscle forces in vivo is one of the most important questions in biomechanics science. However, it is a challenging problem, due to several reasons: actuator redundancy, several kinds of nonlinearities, invasive experimental set ups and ethical difficulties as, for example, installing force sensors in the muscle/tendon directly [1]. Most of the research and clinical works in this field tries to address the problem through one of the following approaches: analysis of joint torques measured by dynamometry or inverse dynamics [2–5], totally predictive simulation (optimal control) [6–8], static optimization [9, 10], direct analysis of the electromyography (EMG) patterns [11], extracted EMG envelopes [12], and EMG-driven models [13, 14]. Each one of these approaches has its own advantages and drawbacks. Blajer et al. [15] has shown how the choice of coordinate system, muscle geometry, number of muscles, and optimization approach influences muscle force estimation in an inverse dynamics analysis, for the upper limb.

This paper discusses some methodological questions regarding the application of EMG-driven models to estimate muscle forces, using as a benchmark an isometric contraction protocol for the *triceps surae* muscle group. The questions addressed include: muscle contraction and activation dynamics formulation, selection, scaling and individual estimation of muscle model parameters, and EMG processing issues. A novel approach based on high-density multichannel EMG is also discussed. Parameter optimization to fit the EMG-driven computed forces to an expected result has been usually avoided, not to mask the effect of model and input processing inaccuracies in the estimated force [13]. This paper summarizes the main observations and conclusions obtained from a series of works carried out recently by our group [16–22]. In total, about 150 experiments have been performed in 40 different subjects. All the experiments were performed in the same conditions within a uniform group of volunteers: normal young adult males between 18 and 19 years old. However, different approaches have been tested comparatively to process the EMG signals, regarding the model formulation and parameter selection or calibration.

2 The isometric triceps surae problem

The addressed biomechanical problem is estimating the plantar flexion isometric torque with the ankle at 90° degrees, knee extended, using a Hill-type muscle model and EMG data (Fig. 1), collected from the three components of *triceps surae* (TS): *gastrocnemius medialis* (GM), *gastrocnemius lateralis* (GL), and *soleus* (SOL) muscles. The main dorsiflexor, *tibialis anterior* (TA), has been also recorded in some tests, to evaluate cocontraction. Ankle joint torque is synchronously recorded from a Cybex^{TM} dynamometer. One of the advantages of using a directly dynamometer-measured joint torque is avoid introducing errors originated from kinematics measurement and dynamic modeling, which are expected to be found in usual inverse dynamics analysis [23].

The directly measured torque is compared to the sum of each muscle force multiplied by the respective ankle moment arm (Fig. 2). The selected subjects has been, in all tests, healthy young adult males (age: 18.6 ± 0.7 years, mass: 65.6 ± 6.0 kg, and height: 173.9 ± 7.8 cm), voluntary from the military personnel enrolled in the basic training program of the Brazilian Army Physical Education School, Rio de Janeiro.

This simple and controlled experiment allows quantifying indirectly the effect of some methodological choices in the torque prediction error. The well-known basic idea of the EMG-driven model approach consists of collecting EMG signals, which are filtered, rectified and input in a muscle dynamical model (Fig. 2). In practice, to apply such a method,

Fig. 1 Experimental setup

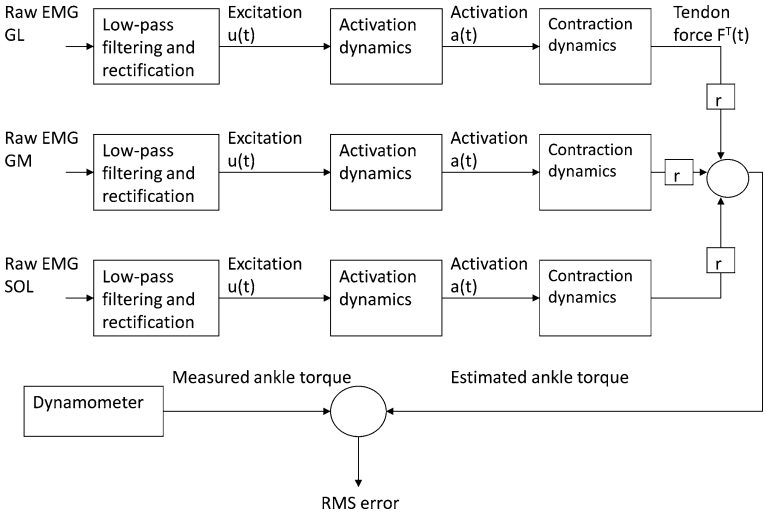

Fig. 2 EMG to muscle force processing and joint torque comparing using a EMG-driven model

several decisions must be made, regarding: EMG electrodes placement, EMG input normalization, filters shape, as well as formulating the activation and contraction dynamics equations, and selecting their parameters. By choosing a functional and anthropometric uniform group of subjects, we have tried to minimize, up to some extent, the possible number of such methodological decisions.

The experimental protocol consists of two plantar flexion isometric contraction steps, separated by a relaxing interval. Each step corresponds to 20% and 60% of the individual Maximum Voluntary Contraction (MVC) torque, which must be tentatively maintained constant through 10 seconds. The subject tries to follow the step target by means of a visual

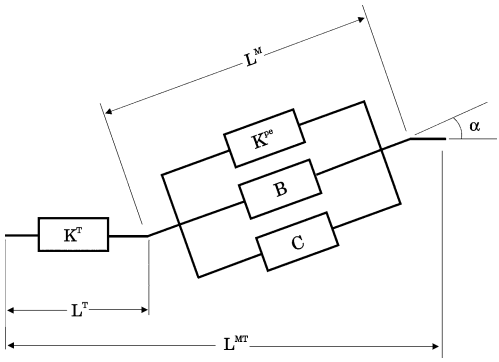

Fig. 3 Musculotendon model of contraction dynamics. C: contractile element, B: damping element, K^{PE}: parallel elastic element, K^T: tendon, L^{MT}: musculotendon length, L^T: tendon length, L^M: muscle length

real-time visual feedback of the actual produced torque, superimposed over a mask of the target in the computer screen [16, 20] (the protocol can be visualized in Fig. 4). Raw EMG signal was initially band-pass filtered (15–350 Hz), rectified, and low-pass filtered with a 2nd order digital Butterworth filter (2 Hz cut-off frequency). Input excitation signal $u(t)$ for the muscle dynamics model was found by normalizing the collected EMG signals with MVC EMG.

Muscle activation dynamics from [24] was used. Contraction dynamics is a modified version of Zajac musculotendon actuator [25] with added parallel elastic and damping elements [16] (Fig. 3). Each muscle is modeled as a system of three differential equations:

$$\begin{aligned} \dot{\underline{a}} &= (u - \underline{a})(k_1 u + k_2) \\ \dot{\tilde{F}}^T &= \tilde{k}^T \left(\tilde{v}^{\mathrm{MT}} - \tilde{v}^M \cos\alpha \right) \\ \dot{\tilde{L}}^M &= \tilde{v}^M \end{aligned} \tag{1}$$

where $\underline{a}$ is the neural activation, u the excitation input signal, k_1 and k_2 time constants, F^T tendon force, k^T tendon stiffness, v^{MT} musculotendon velocity, v^M contractile element velocity, α pennation angle, and L^M contractile element length. The $\sim$ upperscript means that the variables are adimensionalized (see details of notation in [25]). v^{MT} can be considered also as an external input, when the muscle dynamics is integrated independently of the skeletal system associated rigid body dynamics. The relationship between v^M and F^T is modeled using the Hill hyperbole, scaled by the activation level [16]. L^M has been included explicitly as a state variable, since it is used to find the position on the force-length curve that scales maximum muscle force, as well as to find the actual pennation angle (3). The second-order nonlinear dynamic model is integrated numerically using $u(t)$ as the input signal. The initial values for the state variables $\underline{a}$ and F^T has been estimated as the mean normalized EMG activity in the first second of recording. In the case of the contractile element length, the initial value was estimated from OpenSim for the knee extended and ankle at neutral position. It has been observed a high sensitivity of model response with relation to muscle length initial condition.

The estimated torque output was calculated as the sum of each simulated muscle force multiplied by its respective ankle angle moment arm regression equations from [26]. TA moment arm was considered negative, since it is a dorsiflexor muscle. The differences between simulated and Cybex™ measured torques were calculated as the normalized Root

Mean Square Error (%RMSE) between the two curves (2),

$$\%\mathrm{RMSE} = \frac{1}{\mathrm{TM}_{\mathrm{MAX}}}\sqrt{\frac{\sum_{i=1}^{N}(\mathrm{TM}(i)-\mathrm{TS}(i))^2}{N}} \times 100\% \tag{2}$$

where TM is the Cybex$^{\mathrm{TM}}$ measured torque, TS the simulated torque, N the number of samples in the time series, and $\mathrm{TM}^{\mathrm{MAX}}$ the maximum dynamometer measured torque at MVC for each subject. $\mathrm{TM}^{\mathrm{MAX}}$ can be selected either from the absolute maximum or from an average value in the vicinity of the maximum torque (see Sect. 6). The time window considered in the %RMSE calculus can be either the entire protocol (50 s) or each step separately (10 s), to assess the model accuracy in a wider or in a more specific level of activation.

3 The nominal parameters case

One of the most critical decisions to formulate an EMG-driven model problem is choosing the sources of the muscle model parameters. The first and simplest possibility is taking them from one of the several available literature data sources, e.g., [27, 28]. Here, we call "nominal parameters" those available from the "Both Legs" open-source software OpenSim [29] model, which is becoming increasingly popular in the musculoskeletal biomechanics community.

A sample solution of the TS EMG-driven model with nominal parameters is presented in Fig. 4. In the upper part, each muscle contribution to the total torque is shown. In the lower, it is possible to observe the comparison between the estimated and dynamometer measured torques.

The %RMSE torque error distribution for a set of subjects, sorted from smallest to highest, is shown in Fig. 5. Figure 6 presents average results found for the load sharing among the muscles to produce the required torque, for low and medium/high contractions. From these results, some remarks can be highlighted (for a more detailed discussion on the error analysis of these results, see [19]):

(1) Torque error distribution is not Gaussian, even if "normal adult males" are used, which should theoretically correspond, in the mean, to the OpenSim model;
(2) The errors are likely to be toward underestimation;
(3) Model predicts better higher than lower activation levels;
(4) TA contributes little to the cocontraction torque (2–3% of the agonistic), and can usually be disregarded;
(5) A load sharing pattern among the muscles can be observed, following the order: SOL, GM, and GL. However, significant changes in the individual muscle contributions can be observed when load increases. Particularly, GL participation grows with contraction intensity;
(6) The load sharing dispersion among subjects, shown in Fig. 5 error bars as pattern deviations, reduces with load increase.

4 Use of individual muscle model parameters

One possible way to improve model accuracy is by using individual muscle parameters, instead of mean values from literature. Static optimization can be used to adjust some parameters such as maximum muscle force, tendon slack length, and optimal length [13, 30, 31].

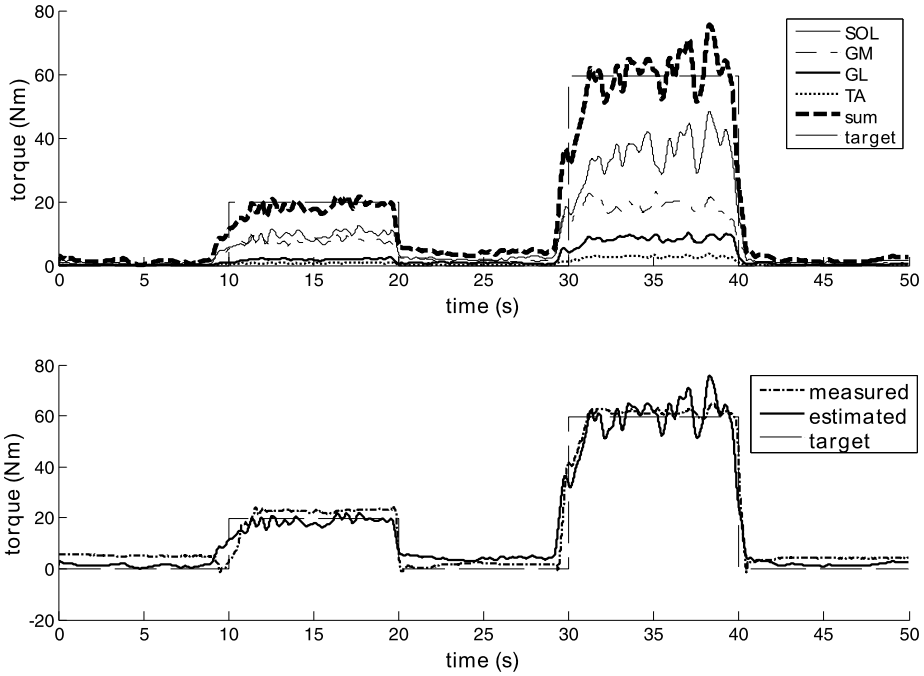

Fig. 4 Sample of the torque matching between EMG-driven model and dynamometer. *The upper graph* shows the individual torque contributions and *the lower* the total joint torque compared to dynamometer measurements

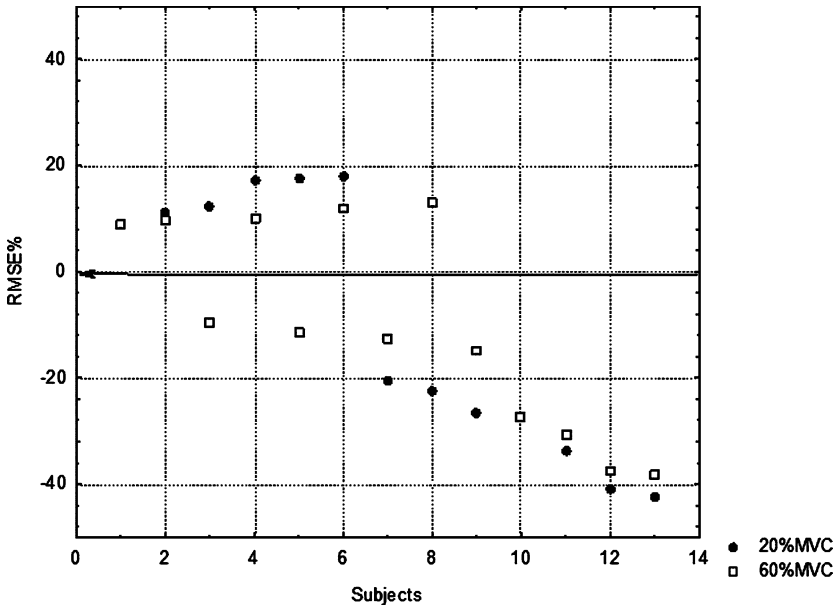

Fig. 5 %RMSE distribution. The subjects (1–13) are ordered from lower to greater error

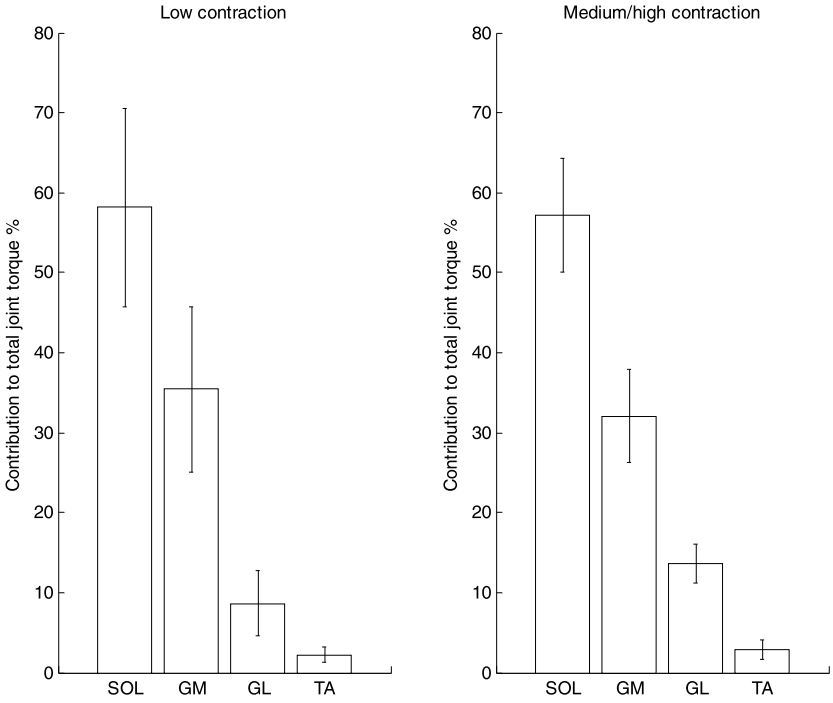

Fig. 6 Contribution of each component of *triceps surae* and *tibialis anterior* to the total ankle torque in low (20%MVC) and medium/high isometric contractions (60%MVC)

Buchanan et al. [32] suggest dividing measured joint torques among the muscles, weighted by the individual PCSAs. Manal and Buchanan [33] propose a specific method to estimate tendon slack length. Winby et al. [34] tested several scaling techniques for optimal muscle fiber length and tendon slack length, according to subject size. They observed that a good scaling can be obtained when the scale is able to maintain the muscle operating range in maximal activation.

Initially, we have investigated the effect of applying simple scale factors to the *nominal* literature muscle model parameters [16]. The proposed scaling factors were determined by dividing each individual anthropometrical or functional measurement by the respective mean value of the entire group, composed of 20 volunteers in this particular study. Maximal muscle force (F^{om}) was scaled by Maximum Torque, Tendon Slack Length by Leg Length, and Moment Arm (r) by Bimalleolar Diameter (Table 1, from [16]). It can be observed that maximum torque scaling reduces significantly %RMSE torque prediction error, while the other proposed scaling factors separately have shown no effect on prediction accuracy. However, when applied altogether decreased error dispersion among the subjects.

An alternative way to find individual muscle parameters is using ultrasound (US) to estimate muscle maximum force (F^{om}) [20]. This imaging technique is used to measure muscle thickness, which allows evaluating *triceps surae* muscle volume, through regression equations from literature [35]. SOL, GM, and GL PCSAs are estimated using published volume proportions among leg muscles [36], which also require measurements of muscle fiber length and pennation angle during rest, made by US (Fig. 7). F^{om} values obtained by this approach were used to test the EMG-model torque prediction accuracy, comparatively to the

Table 1 Torque RMS Errors calculated for the whole protocol time window, when applying scale factors,. NC = No Correction; TM_{MAX} = Maximum Measured Torque; BD = Bimalleolar Diameter; LL = Leg Length; ALL = All corrections applied simultaneously. ANOVA main effect $p = 0.046$. Post-hoc between NC and TM_{max} $^{*}p = 0.046$ and between NC and ALL $^{**}p = 0.026$

Scaling factor	Means(SD)	RMSE(%)(SD)	RMSE(%)(min–max)
NC	–	12.92(4.94)	7.11–25.74
TM_{MAX} (Nm)	104.15(18.53)	10.32(2.06)*	7.17–21.68
BD (cm)	7.19(0.47)	12.19(4.37)	6.83–25.94
LL (cm)	41.13(2.78)	12.94(5.04)	8.01–16.56
ALL	–	10.12(1.73)**	7.98–13.04

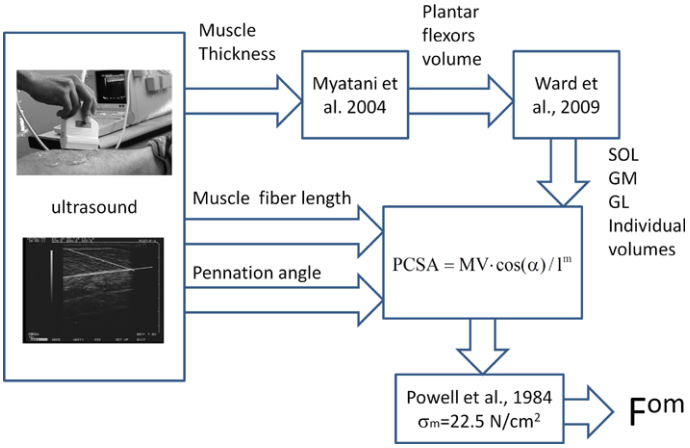

Fig. 7 Procedure adopted to estimate maximum muscle force from US thickness, fiber length, and pennation angle measurements

nominal parameters case. A small but statistically significant reduction in the Root Mean Square Error was observed when US-obtained F^{om} was used, as compared to the F^{om} from literature. Most of the error decrease occurred in the volunteers whose anthropometrical parameters and strength varied more widely from OpenSim data.

It is worth noting that, in this work, an experimentally estimated value of muscle maximum tension $\sigma_m = 22.5$ N/cm^2, as found by Powell et al. [37], was applied. In the nominal OpenSim model, PCSAs from old cadaveric specimens available in literature was used, associated with adjusted values of σ_m, which varied from 73 N/cm^2 to 30 N/cm^2, depending on the PCSA source used [38], as already pointed out by Buchanan [32, 39] and Lloyd and Bessier [13]. Such values of σ_m could not be adopted if PCSA is estimated individually in vivo by US or any other medical image technique. In addition, trained subjects are likely to show an increase in muscle PCSA compared to untrained, but this hypertrophic effect is not sufficient, in many cases, to explain the entire force increase that is usually observed [40]. Part of strength gain can be attributed to neural drive facilitations and to the change of other muscle architecture parameters [41]. Therefore, using specific σ_m values, estimated from MVC experiments for either trained and untrained subjects, is a promising approach, that is now being investigated [42].

5 Model improvements

Two approaches to improve musculotendon dynamics have been tested: using a non-linear formulation for activation dynamics and a muscle-length variable pennation angle [21]. Based on published steady-state EMG-to-force relationships [43], Manal and Buchanan [44] proposed an nonlinear algebraic expression between the "muscular activation" $a(t)$ and "neural activation" $a(t)$, known as "A-Model" (Fig. 8). The classical first-order differential bilinear equation [24] is still used, but a neural-activation dependent nonlinear relationship scales its output. This curve is composed by a logarithmic and a linear part, but is continuous and differentiable throughout the dominion (Fig. 9). Such condition is achieved by formulating and solving numerically (Newton–Raphson) a nonlinear algebraic condition that holds for the node point between the two parts of the curve. For small values of the A parameter, the "nonlinearization" is almost negligible, but for greater values the curve gets more bulged toward the small activation part.

These characteristics are convenient in our particular case, since it has been observed that the torque errors are predominantly of underestimation, especially at small activation levels. In a study performed over 11 subjects, the best A (minimum torque error) values were found among 0.025 and 0.1 (mean 0.07 ± 0.05). By applying this correction, the mean torque errors decreased from $24.13 \pm 10.33\%$ to $12.73 \pm 4.10\%$. On the other hand, the A-model approach implies the introduction, in the activation dynamics formulation, of a certain kind of parameter optimization, what is, a priori, an inconvenient feature in the context of the present studies.

The other model improvement was using a variable pennation angle, instead of a fixed nominal value. Such modification can more accurately represent what actually happens in the physiological system [13, 32]. We have tested the classical formula to estimate the pennation angle:

$$\alpha\left(\tilde{L}^M\right) = \sin^{-1}\left(\frac{\sin(\alpha_o)}{\tilde{L}^m}\right) \tag{3}$$

where $\tilde{L}^M$ is the contractile element normalized length (relative to the optimum length) and α_o the pennation angle at the optimum length. However, this equation is no longer valid if $\sin(\alpha_o) > \tilde{L}^m$, what may occurs if the muscle is highly shortened.

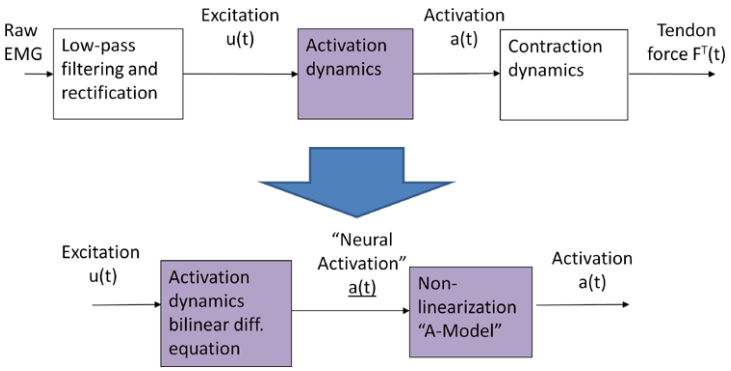

Fig. 8 A-Model activation dynamics. *In the upper part*, the usual activation dynamics formulation is shown, delivering the activation signal from the neural excitation. The A-Model introduces an additional processing step. The result of the classical activation dynamics is called "neural activation," which is algebraically nonlinearized to produce the muscular activation

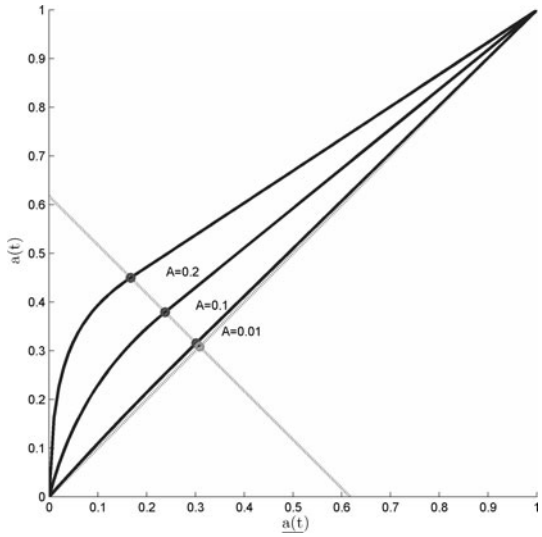

Fig. 9 A-Model relationship between neural activation ($\underline{a(t)}$) and muscular activation $a(t)$. The value of the A-parameter determines the function degree of curvature. Three A parameter values are shown. If $A = 0$, the relationship is one-to-one

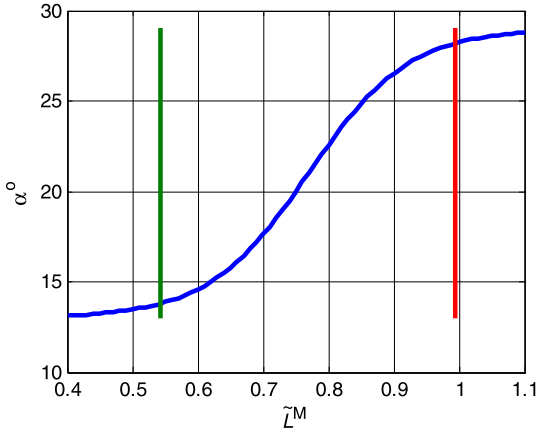

Fig. 10 Exponential curve of variable pennation angle for *gastrocnemius lateralis*, as function of the normalized muscle contractile element length

In our approach, the maximum and minimum contractile elements lengths of the three components of *triceps surae* were estimated from OpenSim. Such length values were them associated to the maximum and minimum pennation angles of each muscle, measured by Kawakami et al. [45]. Between the two points [minimum length, minimum α] [maximum length, maximum α] a smooth exponential curve was adjusted to simulate the intermediary points (Fig. 10, for GM as an example):

$$\alpha\left(\widetilde{L^M}\right) = \frac{\Delta\alpha}{(1 + e^{-\beta(\widetilde{L^M} - \overline{\overline{L^M}})})} + \alpha_{\min} \tag{4}$$

In the above equation, $\Delta\alpha$ is the observed pennation angle amplitude, $\overline{\overline{L}}^M$ is the mean length value, β imposes the curve inclination, and $\alpha_{\min}$ is the minimum value of the pennation angle for each particular muscle.

This model has been used to study comparatively the "benchmark" case, with knee fully extended, to the situation with knee flexed at 90° [21]. In this position, it is expected the *gastrocnemii* to become shortened, and contribute only marginally to the total plantar flexor torque. Therefore, the ankle should behave as a single-muscle joint, and torque readings directly associated to muscle force, which is a very attractive situation for muscle biomechanics studies. The resulting torque sharing patterns among the three muscles, in this particular study were found as: knee extended, SOL, GM, GL percentile contributions to the total torque were (MEAN±SD): 52.8 ± 6.2, 29.2 ± 5.6, and 17.9 ± 3.5, respectively, for all conditions. For the knee flexed, such proportions were 74.9 ± 5.0, 10.0 ± 3.3, and 15.4 ± 3.5. It means that about 25% of the ankle torque is still being produced by the *gastrocnemii*, and the "single muscle paradigm" must be interpreted carefully. However, further knee flexion (e.g., 120°) is likely to reduce GM and GL forces, remaining almost only the *soleus* as the active plantar flexor [46].

6 EMG input issues

Surface EMG signals acquisition and processing are critical questions to be addressed towards more reliable force estimation with EMG-driven models. Excitation $u(t)$ to the EMG-driven model corresponds to the processed EMG signals normalized by the EMG recorded during maximal voluntary isometric (MVC) test. The EMG epoch chosen for MVC reference can constitute itself an error source. The EMG-RMS peak amplitude is a common option, but also a problematic choice due to the high signal variability. Mean RMS value of the whole test period is an alternative. Our group adopts the average RMS of a 2 seconds epoch, chosen visually in the vicinity where the torque curve, given by the dynamometer, is approximately maximal and constant.

The difficulty for fixing the foot to get reliable ankle torque measurements is reported by some authors, e.g., [47]. This is a subtle question: if the rear foot disconnects from the dynamometer support, the ankle joint extends, the muscles from *triceps surae* shorten, and the force at maximum excitation occurs even farther from the optimal length, observed at about 20° of dorsiflexion in static conditions (simulated with OpenSim). If the heel extends during MVC, due to the high forces, but not in submaximal contractions (20% and 60% MVC), the modeled relationship between normalized $u(t)$ and force could fail, due to an unreliable normalization. With this potential problem in mind, we used a custom-made rear heel u-shape apparatus to fix the foot to the dynamometer. It is possible that for some subjects, the foot positioning precaution resulted not completely worthy.

Some MVC tests were also performed with the ankle at 15° of dorsiflexion since, at this position, *triceps surae* produces the highest torque. Indeed, the plantar flexion torque was significantly higher (154.6 ± 12.82 Nm and 110.1 ± 14.63 Nm for dorsiflexed and neutral (0°) ankle positions, respectively) . However, we have observed that EMG maximal amplitudes were similar in both ankle positions, with the same effect for input signal normalization purposes.

Another question that should be worth noting is the most appropriate signal processing technique for extracting the EMG envelope to find the control signal $u(t)$. It can observed that even using a very low cut-off frequency (2 Hz) low-pass filter, large muscle force fluctuations are still observed (for example, the 60% MVC step in Fig. 4). A possible approach for improving such envelope estimation is using more advanced signal processing techniques for envelope-extracting [12, 48] and smoothing [49] to find $u(t)$.

6.1 Use of high-density surface EMG

EMG signals constitute a summation of the motor unit action potentials, occurring within the detection area of the electrode. Constructive and destructive wave superimpositions are present simultaneously, leading to a "natural" large variance of the EMG's linear envelope [47], which does not strictly represent fluctuations in muscle activation. Electrodes positioning about the innervate zone can affect drastically the signal amplitude, as well as the conductor volume, which depends on the distance between the signal origin and the detection system, varying among the anthropometric characteristics of each subject. The use of single differential configuration may hinder force prediction due to the small detection area covered by a couple of electrodes [50, 51], failing to represent the actual excitation $u(t)$ for the muscle as a whole, as hypothesized by the model. However, reliable detection of surface EMG from several electrodes represents a difficult technical problem, since the recording signal has two spatial and one temporal dimension.

A grid of densely spaced monopolar electrodes, known as high-density EMG (HD-EMG) [51, 52], maps the myoelectrical activation over a wide surface on the skin, providing a better spatial representation of the neuromuscular activity. Using spatially distributed electrodes, likely covering different motor units, have shown to increase muscle force estimation accuracy in some EMG-force studies, without concerning to Hill-type muscle models [12, 53]. For example, a 30% improvement of force estimation for the *triceps brachii* muscle during three different contractions levels [53].

Our group, in collaboration with the Laboratory of Engineering of Neuromuscular System of the Politecnico di Torino (LISiN), compared the torque prediction accuracy of HD EMG with the traditional bipolar configuration in the EMG-driven model. A study with 10 adult male subjects, and a similar plantar flexion protocol, was performed [17]. The electrode arrays were: for GM, 6×5 electrodes, 8 mm interelectrode distance (IED); for GL, 8×1 electrode array, 5 mm IED and for SOL, 5×13 electrodes array, 8 mm IED (Fig. 11). For each muscle, the EMG signals were processed in two ways. (1) HD (High Density): the envelopes of single differential EMG signals, pertaining to pairs of electrodes disposed along each column of the matrix, were averaged into a single envelope. (2) BP (bipolar): one single differential signal was digitally obtained between two selected electrodes, separated by 2.4 cm, to simulate the conventional bipolar configuration. In both conditions, the resulting envelope was normalized and input into the model as the excitation signal for each muscle.

The ultrasound device was used to scan both *gastrocnemii* and *soleus* to find the locations for positioning the electrode arrays. Marks on the skin are drawn, according to muscle fibers arrangement, Achilles tendon insertion, and both of the *gastrocnemii* myotendinous junctions (MYJ). The arrays of electrodes were placed at specific locations on the skin following the criteria: (a) GM: longitudinally just over the end of the superficial fibers, laterally one centimeter from the *gastrocnemius* midline, (b) GL: over the line between the MYJ and the end of the superficial fibres, and (c) SOL: just under the medial gastrocnemius myotendinous junction, with the electrode matrix center aligned according to the *gastrocnemius* midline and the Achilles tendon insertion.

The mean RMSE(%) values were: for 20% MVC, 22.2 ± 7.2 and for 60% MVC, 25.7 ± 9.9 with the BP configuration. With HD, the 60% MVC error reduced significantly to 21.6 ± 10.2, showing that the HD-EMG improved the torque estimation error by approximately 16%. The 20% MVC error reduction, to 21.0 ± 8.0 with HD, was not significant.

The choice to use one mean enveloped signal from the electrode matrixes, as representative of the muscle input signal $u(t)$, may perhaps represent not the most appropriate approach. The advantage of the HD-EMG is related to the ability to map the myoelectrical

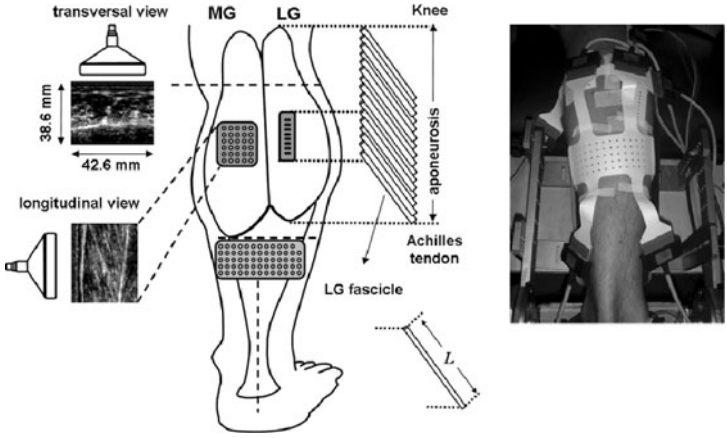

Fig. 11 Schematics of electrodes positioning. *In the left*, the ultrasound images are used to find the anatomical landmarks considered as references for electrodes array positioning. L is the measured fiber length. *On the right*, the electrode array developed by LISiN for the gastrocnemius is shown

activation over a wide superficial area. Therefore, it should be possible to identify areas from which the "most representative" EMG signals can be detected, thus increasing the reliability of the muscle activation level detection. It is possible that averaging the signals, in order to obtain one average signal, have somehow worsened the input function: if the superficial muscle activation is not equally distributed, larger nonactivated areas could pull down the mean signal amplitude; other processing methods, as maximal centroid amplitude and cluster analysis might enhance muscle activation level and force estimations.

7 Conclusions

This paper has addressed some methodological questions regarding the use of an EMG-driven model to estimate isometric ankle muscle forces. Force prediction accuracy can be evaluated indirectly, through the RMS error between the torque curves obtained by the model and those measured synchronously by a dynamometer. Despite the apparent simplicity of the proposed problem, several questions can be raised, especially: the origin and reliability of the muscle dynamical model parameters, some characteristics of muscle dynamics formulation, and EMG input issues. On the average, among the subjects, the prediction was more accurate in medium/high activation than in low activation levels. Usually, the error was of torque underestimation, which can be minimized by applying a nonlinear formulation of activation dynamics (A-Model). A pattern of individual contributions to the total torque has been observed, following the sequence: SOL, GM, and GL. When the activation level increases, GL participation in the torque sharing becomes significantly higher. Simultaneously, intersubject variability of the torque sharing among the muscles decreases. *Tibialis anterior* antagonist has shown little activity in the studied task, and its action can be usually disregarded. Using high density, multichannel EMG has shown to reduce torque estimation error, but at the expense of much greater instrumentation complexity.

Many of these questions must be addressed and better understood, before applying the EMG-driven model approach to other muscle groups, with even more reason in complex

tasks. Increasing model reliability may lead to narrowing system constraints, when optimization techniques are applied to refine the solution. In such situations, we believe that physiologically more meaningful solutions are likely to be obtained.

Acknowledgements The authors gratefully acknowledge CAPES (Coordenadoria de Aperfeiçoamento de Pessoal de Nível Superior) for financial support of the "Muscle Biomechanics Cooperation Network," to FAPERJ (Fundação de Amparo à Pesquisa do Estado do Rio de Janeiro), CNPq (Conselho Nacional de Desenvolvimento Científico e Tecnológico), and IPCFEx (Physical Education Research Institute of the Brazilian Army).

References

1. Fleming, B.C., Beynnon, B.D.: In Vivo measurement of ligament/tendon strains and forces: a review. Ann. Biomed. Eng. **32**, 318–328 (2004)
2. Yeadon, M.R., King, M.A., Wilson, C.: Modeling the maximum voluntary joint torque/angular velocity relationship in human movement. J. Biomech. **39**, 476–482 (2006)
3. Anderson, D.E., Madigana, M.L., Nussbaum, M.A.: Maximum voluntary joint torque as a function of joint angle and angular velocity: model development and application to the lower limb. J. Biomech. **40**, 3105–3113 (2007)
4. Thelen, D.G., Schultz, A.B., Alexander, N.B., Ashton-Miller, J.A.: Effects of age on rapid ankle torque development. J. Gerontol. **51A**(5), M226–M232 (1996)
5. DeVita, P., Hortobagyi, T.: Obesity is not associated with increased knee joint torque and power during level walking. J. Biomech. **36**, 1355–1362 (2003)
6. Menegaldo, L.L., Fleury, A.T., Weber, H.I.: Biomechanical modeling and optimal control of human posture. J. Biomech. **36**, 1701–1712 (2003)
7. Anderson, F.C., Pandy, M.G.: Dynamic optimization of human walking. J. Biomech. Eng. **123**, 381–391 (2001)
8. Ackermann, M., van den Bogert, A.J.: Optimality principles for model-based prediction of human gait. J. Biomech. **43**, 1055–1060 (2010)
9. Yamaguchi, G.T., Moran, D.W., Si, J.: A computationally efficient method for solving the redundant problem in biomechanics. J. Biomech. **28**, 999–1005 (1995)
10. Bottasso, C.L., Prilutsky, B.I., Croce, A., Imberti, E., Sartirana, S.: A numerical procedure for inferring from experimental data the optimization cost functions using a multibody model of the neuromusculoskeletal system. Multibody Syst. Dyn. **16**, 123–154 (2006)
11. Beck, T.W., DeFreitas, J.M., Stock, M.S., Dillon, M.A.: Comparison of the muscle activation pattern for the vastus lateralis before and after an 8-week resistance training program. Biomed. Signal Process. Control **5**, 264–270 (2010)
12. Clancy, E.A., Hogan, N.: Multiple site electromyography amplitude estimation. IEEE Trans. Biomed. Eng. **42**, 203–211 (1995)
13. Lloyd, D.G., Besier, T.F.: An EMG-driven musculoskeletal model to estimate muscle forces and knee joint moments in vivo. J. Biomech. **36**, 765–776 (2003)
14. Langenderfer, J., LaScalza, S., Mell, A., Carpenter, J.E., Kuhn, J.E., Hughes, R.E.: An EMG-driven model of the upper extremity and estimation of long head biceps force. Comput. Biol. Med. **35**, 25–39 (2005)
15. Blajer, W., Czaplicki, A., Dziewiecki, K., Mazur, Z.: Influence of selected modeling and computational issues on muscle force estimates. Multibody Syst. Dyn. **24**, 473–492 (2010)
16. Menegaldo, L.L., Oliveira, L.F.: Effect of muscle model parameter scaling for isometric plantar flexion torque prediction. J. Biomech. **42**, 2597–2601 (2009)
17. Oliveira, L.F., Vieira, T.M.M., Menegaldo, L.L., Merletti, R.: Can the use of a high density EMG system improve a biomechanical model for predicting ankle plantar flexors force. In: Proceedings of 22th ISB Congress, Cape Town, South Africa (2009)
18. Oliveira, L.F., Menegaldo, L.L.: Study of muscle torque sharing patterns in isometric plantar flexion by an EMG-driven biomechanical model. In: Proceedings of the Annual Meeting of the American Society of Biomechanics, State College, PA (2009)
19. Oliveira, L.F., Menegaldo, L.L.: Input error in an EMG-driven muscle model: an analysis based on isometric plantar flexion (2011 submitted)
20. Oliveira, L.F., Menegaldo, L.L.: Individual-specific muscle maximum force estimation using ultrasound for ankle joint torque prediction using an EMG-driven Hill-type model. J. Biomech. **43**, 2816–2821 (2010)

21. Menegaldo, L.L., Oliveira, L.F.: Plantar flexors isometric force distribution patterns with the knee extended or flexed. In: Abstracts of 6th World Congress of Biomechanics, Singapore (2010)
22. Oliveira, L.F., Menegaldo, L.L.: Torque sharing in submaximal isometric plantar flexion: an analysis based on an EMG-driven muscle model. In: Proceedings of XXII Brazilian Congress on Biomedical Engineering, Tiradentes, Brazil (2010)
23. Silva, M.P.T., Ambrósio, J.A.C.: Kinematic Data Consistency in the Inverse Dynamic Analysis of Biomechanical Systems. Multibody Syst. Dyn. **8**, 219–239 (2002)
24. Piazza, S.J., Delp, S.L.: The influence of muscles on knee flexion during the swing phase of gait. J. Biomech. **29**, 723–733 (1996)
25. Zajac, F.E.: Muscle and tendon: properties, models, scaling and application to biomechanics and motor control. CRC. Crit. Rev. Biomed. Eng. **17**, 359–411 (1989)
26. Menegaldo, L.L., Fleury, A.T., Weber, H.I.: Moment arms and musculotendon lengths estimation for a three-dimensional lower-limb model. J. Biomech. **37**, 1447–1453 (2004)
27. Brand, R., Crowninshield, R., Wittstock, C., Pedersen, D., Clark, C., Van Frieken, F.: A model of lower extremity muscular anatomy. J. Biomech. Eng. **104**, 304–310 (1982)
28. Wickiewicz, T.L., Roy, R.R., Powell, P.L., Edgerton, V.R.: Muscle architecture of the human lower limb. Clin. Orthop. Relat. Res. **179**, 275–283 (1983)
29. Delp, S.L., Anderson, F.C., Arnold, A.S., Loan, P., Habib, A., John, C., Guendelman, E., Thelen, D.G.: OpenSim: open-source software to create and analyze dynamic simulations of movement. IEEE Trans. Biomed. Eng. **54**, 1940–1950 (2007)
30. Garner, B.A., Pandy, M.G.: Estimation of musculotendon properties in the human upper limb. Ann. Biomed. Eng. **31**, 207–220 (2003)
31. Redl, C., Gfoehler, M., Pandy, M.G.: Sensitivity of muscle force estimates to variations in muscle–tendon properties. Hum. Mov. Sci. **26**, 306–319 (2007)
32. Buchanan, T.S., Lloyd, D.G., Manal, K., Besier, T.F.: Neuromusculoskeletal modeling: estimation of muscle forces and joint moments and movements from measurements of neural command. J. Appl. Biomech. **20**, 367–395 (2004)
33. Manal, K., Buchanan, T.S.: Subject-specific estimates of tendon slack length: a numerical method. J. Appl. Biomech. **20**, 195–203 (2004)
34. Winby, C.R., Lloyd, D.G., Kirk, T.B.: Evaluation of different analytical methods for subject-specific scaling of musculotendon parameters. J. Biomech. **41**, 1682–1688 (2008)
35. Miyatani, M., Kanechisa, H., Ito, M., Kawakami, Y., Fukunaga, T.: The accuracy of volume estimates using ultrasound muscle thickness measurements in different muscle groups. Eur. J. Appl. Physiol. **91**, 264–272 (2004)
36. Ward, S.R., Eng, C.M., Smallwood, L.H., Lieber, R.L.: Are current measurements of lower extremity muscle architecture accurate? Clin. Orthop. Relat. Res. **467**, 1074–1082 (2009)
37. Powell, P.L., Roy, R.R., Kanim, P., Bello, M.A., Edgerton, V.R.: Predictability of skeletal muscle tension from architectural determinations in guinea pig hindlimbs. J. Appl. Physiol. **57**, 1715–1721 (1984)
38. Hoy, M.G., Zajac, F.E., Gordon, M.E.: A musculoskeletal model of the human lower extremity: the effect of muscle, tendon, and moment arm on the moment-angle relationship of musculotendon actuators at the hip, knee, and ankle. J. Biomech. **23**, 157–169 (1990)
39. Buchanan, T.S.: Evidence that maximum muscle stress is not a constant: differences in specific tension in elbow flexors and extensors. Med. Eng. Phys. **17**, 529–536 (1995)
40. Narici, M.V., Roi, G.S., Landoni, L., Minetti, A.E., Cerretelli, P.: Changes in force, cross-sectional area and neural activation during strength training and detraining of the human quadriceps. Eur. J. Appl. Physiol. Occup. Physiol. **59**, 310–319 (1989)
41. Kawakami, Y., Abe, T., Kuno, S.-Y., Fukunaga, T.: Training-induced changes in muscle architecture and specific tension. Eur. J. Appl. Physiol. Occup. Physiol. **72**, 37–43 (1995)
42. Menegaldo, L.L., Oliveira, L.F.: An EMG-driven model to evaluate quadriceps strengthening after an isokinetic training. Procedia IUTAM **2**, 131–141 (2011)
43. Woods, J.J., Bigland-Ritchie, B.: Linear and nonlinear surface EMG/force relationships in human muscles. An anatomical/functional argument for the existence of both. Am. J. Phys. Med. **62**, 287–299 (1983)
44. Manal, K., Buchanan, T.S.: One-parameter neural activation to muscle activation model: estimating isometric joint moments from electromyograms. J. Biomech. **36**, 1197–1202 (2003)
45. Kawakami, Y., Ichinose, Y., Fukunaga, T.: Architectural and functional features of human triceps surae muscles during contraction. J. Appl. Physiol. **85**, 398–404 (1998)
46. Maganaris, C.N.: A predictive model of moment-angle characteristics in human skeletal muscle: application and validation in muscles across the ankle joint. J. Theor. Biol. **230**, 89–98 (2004)
47. Karamanidis, K., Stafilidis, S., DeMonte, G., Morey-Klapsing, G., Bruggemann, G., Arampatzis, A.: Inevitable joint angular rotation affects muscle architecture during isometric contraction. J. Electromyogr. Kinesiol. **15**, 608–616 (2005)

48. Clancy, E.A., Morin, E.L., Merletti, R.: Sampling, noise-reduction and amplitude estimation issues in surface electromyography. J. Electromyogr. Kinesiol. **12**, 1–16 (2002)
49. Alonso, F.J., Del Castillo, J.M., Pintado, P.: Application of singular spectrum analysis to the smoothing of raw kinematic signals. J. Biomech. **38**, 1085–1092 (2005)
50. Farina, D., Merletti, R., Enoka, R.: The extraction of neural strategies from the surface EMG. J. Appl. Physiol. **96**, 1486–1495 (2004)
51. Merletti, R., Holobar, A., Farina, D.: Analysis of motor units with high-density electromyography. J. Electromyogr. Kinesiol. **18**, 879–890 (2008)
52. Cavalcanti Garcia, M.A., Vieira, T.M.M.: Surface electromyography: why, when and how to use it. Rev. Andal Med. Deporte **04**, 17–28 (2011)
53. Staudenmann, D., Kingma, I., Daffertshofer, A., Stegeman, D.F., van Dieen, J.H.: Towards optimal multichannel EMG electrode configurations in muscle force estimation: a high-density EMG study. J. Electromyogr. Kinesiol. **15**, 1–11 (2005)